Journal of Solid State Chemistry **146,** 124–128 (1999)
Article ID jssc.1999.8317, available online at http://www.idealibrary.com on IDEAL®

The Crystal Structure of $Ba_{17}Sm_{10}Cl_{64}$

Guo Liu[1] and Harry A. Eick[2]

Department of Chemistry and Center for Fundamental Materials Research, Michigan State University, East Lansing, Michigan 48824-1322

Received January 20, 1999; in revised form March 25, 1999; accepted April 8, 1999

The structure of $Ba_{17}Sm_{10}Cl_{64}$, prepared by solvolytic extraction of a program-cooled 1:1 $BaCl_2$:$SmCl_3$ molar mixture sealed in a quartz tube and heated to 750°C, was determined from single-crystal X-ray diffraction data. The compound exhibits cubic symmetry, space group *Pa*3 (No. 205) with $a = 21.366(2)$ Å and $Z = 4$. Refinement effected with $I > 2\sigma(I)$ yielded $R_1 = 0.0926$ and $wR_2 = 0.216$. One Ba atom is 12-coordinated by Cl atoms in a distorted icosahedral arrangement; the three other Ba atoms are 10-coordinated in a distorted bicapped cubic arrangement. There are two Sm atom sites. The coordination around one Sm atom is best described as square antiprismatic, but one Sm–Cl distance is too long for effective bonding. The other Sm atom site, occupied statistically by $\frac{1}{3}$Ba and $\frac{2}{3}$Sm atoms, is 9-coordinated by Cl atoms in a monocapped square antiprismatic arrangement. The two types of Sm sites combine to form an M_6Cl_{37} cuboctahedral cluster of the composition $BaSm_5Cl_{37}$. It is shown that the *cβ* phase identified previously in the Yb–F and related fluoride systems is probably isostructural with $Ba_{17}Sm_{10}Cl_{64}$. © 1999 Academic Press

Key Words: **Structure, X-ray; cuboctahedral cluster; mixed-metal halide.**

---

1. INTRODUCTION

Blachnik *et al.* (1) examined several $BaCl_2$–$LnCl_3$ systems by differential thermal analysis and identified three phases for the $Ln = Sm$ system. Their composition–temperature phase diagram suggested the formulas of these phases to be $BaSmCl_5$, Ba_2SmCl_7, and Ba_3SmCl_9. Löchner and Blachnik (2) further characterized the Ba_2SmCl_7 phase and reported that its composition was better represented as $(Sm, Ba)_{15}Cl_{34+x}$. They suggested its fluorite-type superstructure was based upon the M_6X_{37} anion-excess cuboctahedral cluster initially identified by Bevan *et al.* (3), and that its structure was related to that of $R\bar{3}$ $Eu_{14}Cl_{32}O$ (4). Meyer and Masselmann, using an AgCl flux and a 2:1 $BaCl_2$:$SmCl_3$ mixture, confirmed this suggestion and determined the composition of the phase to be $Ba_9[\{Sm_6Z\}Cl_{34}]$, where Z is presumed to be an oxide ion residing in a large hole in the M_6Cl_{36} cluster (5). They also reported the structure of the phase, $Ba_8[\{Sm_6Z\}Cl_{32}]$, prepared from a 1:1 $BaCl_2$:$SmCl_3$ mixture in an AgCl flux (5).

In the course of our studies on solvolytic decomposition reactions of some fused alkaline earth–lanthanide trihalide systems (6), we isolated crystals in the $BaCl_2$–$SmCl_3$ system that exhibited a fluorite-related superstructure. On the basis of a crystallographic structural study, the composition of the crystals was subsequently determined to be $Ba_{17}Sm_{10}Cl_{64}$. We describe the structure herein.

2. EXPERIMENTAL

Crystal Growth

Crystals of $Ba_{17}Sm_{10}Cl_{64}$ were grown by the molten salt method with excess $SmCl_3$ used as flux. Anhydrous $BaCl_2$ and $SmCl_3$ mixed in a 1:1 molar ratio in an argon-filled glove box (typical moisture and oxygen contents of ~0.5 and ~5 ppm_v, respectively), were put into a previously outgassed quartz tube. The tube was removed from the glove box, quickly attached to a vacuum line, evacuated to 10^{-6} Torr, and sealed with a torch. The mixture was heated in a tube furnace to 750°C to form the melt, then cooled to 500°C at 3°C/h, and finally further cooled to room temperature at 10°C/h. The fused salt was crushed with an agate mortar and a pestle in the glove box and then extracted with a Soxhlet extractor by tetrahydrofuran (THF) for about 1 h. The extraction setup and procedure have been described previously (7). The slightly yellowish crystals that remained were dispersed in sodium-dried paraffin oil for microscopic examinations. Appropriate specimens were paper-dried and sealed in capillaries for X-ray diffraction studies.

X-Ray Diffraction Data Collection and Data Processing

Several crystals were screened by the precession method, and most were found to be twinned. A crystal that appeared to be single was transferred to a Nicolet P3F four-circle X-ray diffractometer for further examination and for data

---

[1] Present address: Westaim Advanced Display Technologies, Inc., 15 City View Drive, Toronto, Ontario, Canada M9W 5A5.

[2] To whom correspondence should be addressed.

0022-4596/99 $30.00

collection. Reflection data were obtained with Mo radiation by the ω–2θ scan procedure. Intensity data of four standard reflections measured after every 96 reflections indicated negligible crystal decay. Data reduction and structure solution were performed without applying an absorption correction. Systematic extinctions were consistent only with space group $Pa3$ (No. 205). Most of the Ba and Sm atoms were located initially by direct methods; remaining atoms were located from difference Fourier analyses. Scattering factors of neutral atoms were used. The structure was refined by full-matrix least-squares on F^2 with the program SHELXL (8).

After all the metal and Cl atoms had been located, the chemical formula was established as $M_{27}Cl_{64}$, which is consistent only with the formulation $Ba_{17}Sm_{10}Cl_{64}$. The small difference in the scattering powers of the Ba and Sm atoms made assignment of Ba and Sm sites based only on convergency factors difficult. Fortunately, there is a significant difference between the Ba–Cl and Sm–Cl bond distances. This difference allowed the sites of atoms Ba(1) to Ba(4) and Sm(1) to be distinguished readily. The chemical composition requires that the remaining metal site, labeled Sm(2), be statistically occupied by $\frac{2}{3}$Sm and $\frac{1}{3}$Ba atoms. After these assignments had been made, the refined results were chemically reasonable.

The thermal parameters are well within the normal range even in the absence of an absorption correction. The crystal data are summarized in Table 1, atomic parameters are listed in Table 2, anisotropic thermal parameters in Table 3, and selected bond distances in Table 4.[3]

TABLE 1
Crystal Data and Structure Refinement for $Ba_{17}Sm_{10}Cl_{64}$

Empirical formula	$Ba_{17}Sm_{10}Cl_{64}$
Formula weight	6107.08
Temperature	293(2) K
Wavelength	0.71073Å
Crystal system	cubic
Space group	$Pa3$
Unit cell dimensions	$a = 21.366(2)$ Å
Volume	9754(2) Å^3
Z	4
Density (calculated)	4.159 Mg/m^3
Absorption coefficient	14.413 mm^{-1}
$F(000)$	10,640
Crystal size	0.46 × 0.44 × 0.24 mm
θ-range for data collection	2.13–27.54°
Index ranges	$0 \leq h \leq 27$, $0 \leq k \leq 27$, $-27 \leq l \leq 0$
Reflections collected	11,253
Independent reflections	3761 [$R(\text{int}) = 0.2276$]
Refinement method	Full-matrix least-squares on F^2
Data/restraints/parameters	3760/0/139
Goodness-of-fit on F^2	1.083
Final R indices [$I > 2\sigma(I)$]	$R_1 = 0.0926$, w$R_2 = 0.2156$
R indices (all data)	$R_1 = 0.1219$, w$R_2 = 0.2570$
Extinction coefficient	0.0
Largest diff. peak and hole	4.152 and -5.544 eÅ^3

TABLE 2
Atomic Coordinates ($\times 10^4$) and Equivalent Isotropic Displacement Parameters (Å$^2 \times 10^3$) for $Ba_{17}Sm_{10}Cl_{64}$

	x	y	z	U(eq)
Ba(1)	0	0	0	55(1)
Ba(2)	3195(1)	3195(1)	3195(1)	40(1)
Ba(3)	8277(1)	1781(1)	−123(1)	39(1)
Ba(4)	8257(1)	4832(1)	−92(1)	36(1)
Sm(1)	6662(1)	1638(1)	1514(1)	32(1)
Sm(2)*	6619(1)	3390(1)	18(1)	37(1)
Cl(1)	6651(2)	2826(2)	2205(2)	42(1)
Cl(2)	7402(2)	2484(2)	817(2)	39(1)
Cl(3)	7449(2)	894(2)	750(2)	37(1)
Cl(4)	5881(2)	4154(2)	908(2)	48(1)
Cl(5)	7468(2)	4097(2)	918(2)	43(1)
Cl(6)	6668(2)	456(2)	2107(2)	47(1)
Cl(7)	5914(2)	878(2)	726(2)	38(1)
Cl(8)	5528(2)	1613(2)	2133(2)	49(1)
Cl(9)	5898(2)	2481(2)	842(2)	40(1)
Cl(10)	4148(3)	4148(3)	4148(3)	47(2)
Cl(11)	5333(3)	3327(3)	−329(3)	59(1)
Cl(12)	1425(3)	1425(3)	1425(3)	73(3)

Note. U(eq) is defined as one-third of the trace of the orthogonalized U_{ij} tensor. The Sm(2) site, indicated with an *, is occupied statistically by $\frac{1}{3}$Ba and $\frac{2}{3}$Sm atoms.

3. DISCUSSION

Barium Atom Coordination

The Ba(1) site is coordinated by 12 chlorine atoms in a distorted icosahedral arrangement as shown in Fig. 1. Sites Ba(2), Ba(3), and Ba(4) are all 10-coordinate. The $BaCl_{10}$ polyhedra, one of which is shown in Fig. 2, have similar geometries and can be described as either bicapped cubic coordination or half-cubic, half-icosahedral (9) coordination.

Samarium Atom Coordination

The Sm(1) sites are coordinated by eight chlorine atoms in a square-antiprismatic geometry. The ninth chlorine

---

[3] See NAPS document No. 05522 for 9 pages of supplementary material. This is not a multiarticle document. Order from NAPS c/o Microfiche Publications, 248 Hempstead Turnpike, West Hempstead, New York 11552. Remit in advance in U.S. funds only \$15.00 for photocopies of \$5.00 for microfiche. There is a \$25.00 invoicing charge on all orders filled before payment. Outside U.S. and Canada add postage of \$4.50 for the first 20 pages and \$1.00 for each 10 pages of material thereafter, or \$5.00 for the first microfiche and \$1.00 for each microfiche thereafter.

TABLE 3
Anisotropic Displacement Parameters (Å^2×10^3) for $Ba_{17}Sm_{10}Cl_{64}$

	U_{11}	U_{22}	U_{33}	U_{23}	U_{13}	U_{12}
Ba(1)	55(1)	55(1)	55(1)	13(1)	13(1)	13(1)
Ba(2)	40(1)	40(1)	40(1)	7(1)	7(1)	7(1)
Ba(3)	43(1)	39(1)	37(1)	− 6(1)	6(1)	− 6(1)
Ba(4)	38(1)	35(1)	36(1)	2(1)	2(1)	2(1)
Sm(1)	30(1)	31(1)	35(1)	1(1)	0(1)	0(1)
Sm(2)*	33(1)	33(1)	43(1)	0(1)	2(1)	0(1)
Cl(1)	41(2)	44(2)	40(2)	− 7(2)	− 1(2)	2(2)
Cl(2)	36(2)	38(2)	41(2)	− 3(2)	1(1)	− 4(2)
Cl(3)	37(2)	39(2)	35(2)	0(1)	2(1)	2(2)
Cl(4)	45(2)	53(3)	44(2)	7(2)	− 2(2)	− 7(2)
Cl(5)	44(2)	44(2)	40(2)	5(2)	5(2)	7(2)
Cl(6)	42(2)	42(2)	58(3)	12(2)	− 3(2)	− 2(2)
Cl(7)	35(2)	43(2)	37(2)	0(2)	− 2(2)	2(2)
Cl(8)	41(2)	50(2)	56(3)	− 2(2)	10(2)	− 1(2)
Cl(9)	37(2)	41(2)	41(2)	− 4(2)	− 5(2)	5(2)
Cl(10)	47(2)	47(2)	47(2)	10(2)	10(2)	10(2)
Cl(11)	54(3)	62(3)	60(3)	6(2)	− 11(2)	3(2)
Cl(12)	73(3)	73(3)	73(3)	− 10(3)	− 10(3)	− 10(3)

Note. The anisotropic displacement factor exponent takes the form $-2\pi^2\,[h^2a^{*2}U_{11} + \ldots + 2hka^*b^*U_{12}]$. (See the Table 2 caption for the meaning of the * or the Sm(2) site.)

atom common to the three Sm(1) sites is located at a distance too long to be considered bonding, > 4.4 Å. Coordination around the Sm(2) sites is best described as monocapped square antiprismatic, with the capped site occupied by a chlorine atom common to three Sm(2) antiprisms.

The Cluster

The most significant structure fragment, shown in Fig. 3, is an M_6Cl_{37} cluster ($BaSm_5Cl_{37}$ because of the Sm(2) site occupancy) formed from three Sm(1) and three Sm(2) polyhedra arranged above and below the shared Cl(12) atom which lies on the 3-fold axis. This atom, Cl(12), which is in the middle of the cluster, can only be bonded to atoms in the Sm(2) sites. The Sm(2)–Cl(12) distance is 3.137 Å compared to the shortest Sm(1)–Cl(12) distance of 4.456 Å.

In Fig. 3 the 12 "hatched" chlorine atoms within the cluster define a cuboctahedron. The larger hatched circle located in the cuboctahedron, Cl(12), while on the 3-fold axis, is off-center and closer to the Sm(2) site to which it is bonded. Figure 4 shows a projection of the $BaSm_5Cl_{37}$ cluster as viewed down the 3-fold axis.

The samarium atoms in the cluster are situated in an octahedral arrangement as they would be in the fluorite structure. Thus, a cluster can be formed from an octahedron of metal atoms, and the clusters are isolated from each other.

Related Structures

The cuboctahedral M_6X_{37} cluster was initially identified in numerous mixed metal–fluoride and oxide–fluoride systems and in a few metal–chloride systems. Many fluoride-containing systems, including the calcium yttro–fluorite mineral tveitite (3, 10), in which the cluster was first definitively characterized, are listed in a compilation by Bevan *et al.* (11). These authors list two compounds that contain chloride ions, $Nd_{14}Cl_{33}$ and $Nd_{14}Cl_{32}O$ (11). The cluster was subsequently identified in $Eu_{14}Cl_{33}$ (12), and more recently in $Ba_8[\{M_6Z\}Cl_{32}]$ ($M =$ Pr, Nd, Sm, Eu) and $Ba_9[\{M_6Z\}Cl_{34}]$ ($M =$ La–Nd, Sm, Eu) (5), where Z presumably represents an oxygen atom that is a part of the

TABLE 4
Bond Lengths [Å] for $Ba_{17}Sm_{10}Cl_{64}$

6Ba(1)–Cl(4)	3.251(5)	Sm(1)–Cl(8)	2.761(5)
6Ba(1)–Cl(11)	3.712(6)	Sm(1)–Cl(1)#12	2.803(4)
mean Ba(1)–Cl	3.482(6)	Sm(1)–Cl(9)	2.822(4)
		Sm(1)–Cl(6)	2.826(4)
3Ba(2)–Cl(2)	3.103(4)	Sm(1)–Cl(2)	2.826(4)
3Ba(2)–Cl(5)	3.118(4)	Sm(1)–Cl(3)	2.830(4)
3Ba(2)–Cl(1)	3.498(5)	Sm(1)–Cl(7)	2.833(4)
Ba(2)–Cl(10)	3.53(1)	Sm(1)–Cl(1)	2.937(4)
mean Ba(2)–Cl	3.268(5)	mean Sm(1)–Cl	2.830(4)
Ba(3)–Cl(4)#10	3.100(5)	Sm(2)–Cl(11)#14	2.840(6)
Ba(3)–Cl(9)#10	3.107(4)	Sm(2)–Cl(11)	2.848(6)
Ba(3)–Cl(3)#11	3.122(4)	Sm(2)–Cl(6)#11	2.908(5)
Ba(3)–Cl(2)	3.129(4)	Sm(2)–Cl(8)#10	2.929(5)
Ba(3)–Cl(5)#12	3.151(4)	Sm(2)–Cl(4)	2.961(6)
Ba(3)–Cl(3)	3.193(4)	Sm(2)–Cl(9)	3.040(5)
Ba(3)–Cl(4)#12	3.318(5)	Sm(2)–Cl(5)	3.045(5)
Ba(3)–Cl(6)#11	3.487(5)	Sm(2)–Cl(2)	3.077(4)
Ba(3)–Cl(1)#10	3.522(4)	Sm(2)–Cl(12)#16	3.137(5)
Ba(3)–Cl(8)	3.736(6)	mean Sm(2)–Cl	2.976(5)
mean Ba(3)–Cl	3.287(5)		
Ba(4)–Cl(10)#13	3.135(3)		
Ba(4)–Cl(5)	3.156(5)		
Ba(4)–Cl(7)#11	3.177(4)		
Ba(4)–Cl(9)#14	3.180(4)		
Ba(4)–Cl(7)#14	3.186(4)		
Ba(4)–Cl(3)#15	3.264(4)		
Ba(4)–Cl(7)#15	3.343(5)		
Ba(4)–Cl(6)#11	3.389(5)		
Ba(4)–Cl(11)#14	3.440(6)		
Ba(4)–Cl(8)#11	3.442(5)		
mean Ba(4)–Cl	3.271(5)		

Note. Symmetry transformations used to generate equivalent atoms: #1 $-x+\frac{1}{2},y-\frac{1}{2},z$; #2 $y-\frac{1}{2},z,-x+\frac{1}{2}$; #3 $-y+\frac{1}{2},-z,x-\frac{1}{2}$; #4 $-z,x-\frac{1}{2},-y+\frac{1}{2}$; #5 $x-\frac{1}{2},-y+\frac{1}{2},-z$; #6 $z,-x+\frac{1}{2},y-\frac{1}{2}$; #7 $x-\frac{1}{2},y,-z+\frac{1}{2}$; #8 $-z+\frac{1}{2},x-\frac{1}{2},y$; #9 $y,-z+\frac{1}{2},x-\frac{1}{2}$; #10 $y+\frac{1}{2},z,-x+\frac{1}{2}$; #11 $-z+1,-x+1,-y$; #12 $-z+1,x-\frac{1}{2},-y+\frac{1}{2}$; #13 $x+\frac{1}{2},y,-z+\frac{1}{2}$; #14 $-y+1,z+\frac{1}{2},-x+\frac{1}{2}$; #15 $-x+\frac{3}{2},y+\frac{1}{2},z$; #16 $x+\frac{1}{2},-y+\frac{1}{2},-z$; #17 $-z+\frac{1}{2},-x+1,y-\frac{1}{2}$; #18 $y+\frac{1}{2},-z+\frac{1}{2},-x+1$; #19 $-y+1,-z,-x+1$; #20 $-x+\frac{3}{2},y-\frac{1}{2},z$.

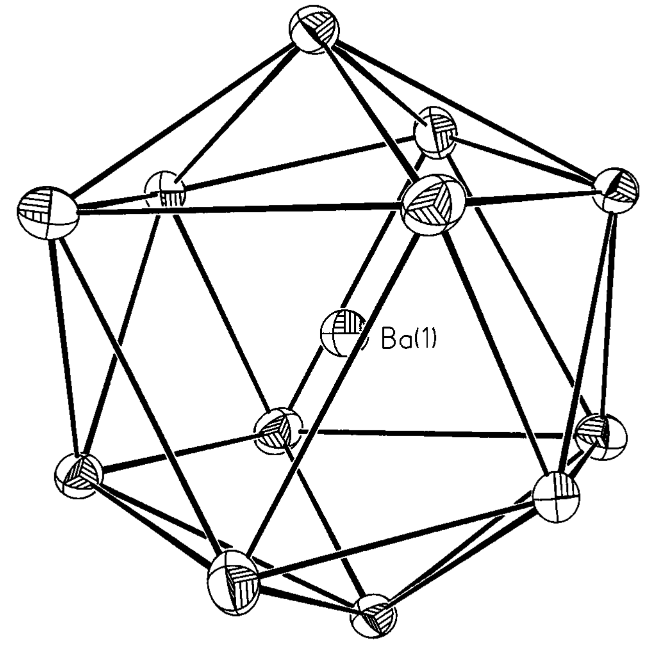

FIG. 1. The $Ba(1)Cl_{12}$ coordination polyhedron showing distorted icosahedral geometry.

cluster. (Compounds in which M = Eu also contained Eu^{II} ions on the Ba site.) The cluster has also been observed in related bromide structures: $Ba_8[\{M_6Z\}Br_{32}]$ (M = Ce–Nd) and $Ba_9[\{M_6Z\}Br_{34}]$ (M = La–Sm) (13).

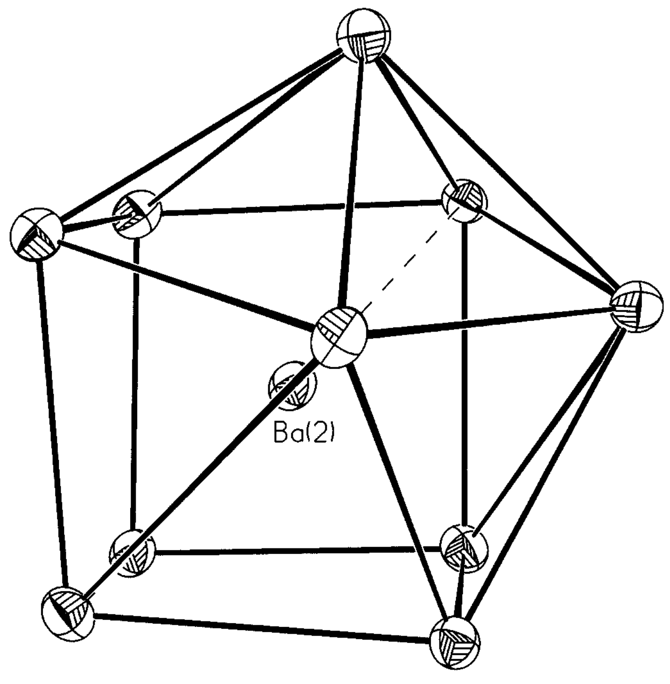

FIG. 2. The irregular bicapped cubic $Ba(n)Cl_{10}$ (n = 2, 3, 4) coordination polyhedron.

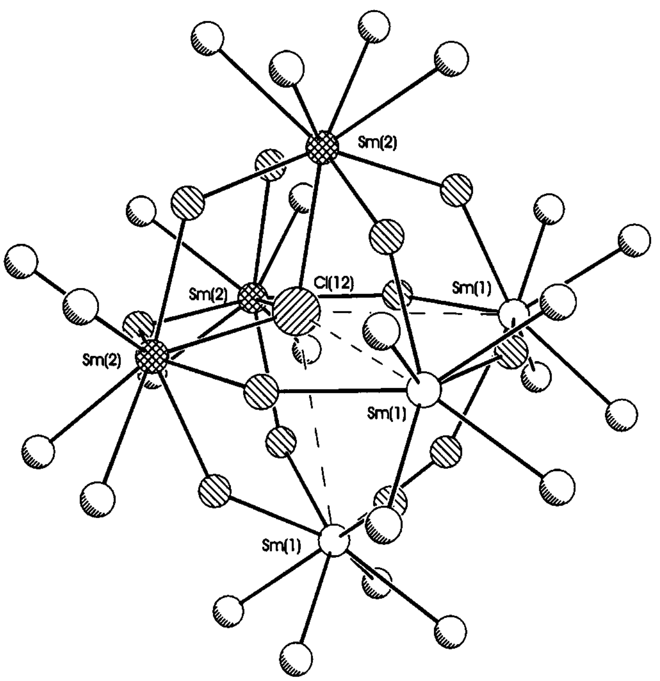

FIG. 3. The geometry of a $BaSm_5Cl_{37}$ cluster group showing the 9-coordinated, monocapped square antiprismatic $Sm(2)Cl_9$ polyhedra and the $Sm(1)Cl_8$ square antiprisms. The Sm(2) site is statistically occupied by $\frac{2}{3}Sm^{III}$ and $\frac{1}{3}Ba^{II}$; the hatched 12 small circles (Cl atoms) form a cuboctahedron with an off-center Cl atom in the middle.

The structures of Ba_2MCl_7 (M = Y, Gd–Yb) (14) are monoclinic with the M atom surrounded by 7 chlorine atoms arranged in a trigonal prismatic fashion with a capped rectangular face, indicative that the radius of these heavier lanthanides must be less than that required to stabilize the cuboctahedral cluster.

Greis found numerous fluorite-related phases in the MF_2–MF_3 systems, where M represents the common divalent lanthanides Sm (15), Eu (16), and Yb (17). One phase with the formula $MF_{2.370}$ ($M_{27}F_{64}$), which he designated as $c\beta$, was common to these systems and was also found with mixed cations, $Sm_{17}Eu_{10}F_{64}$ (16). The composition of this phase is similar to that of $Ba_{17}Sm_{10}Cl_{64}$, suggestive that the phases might be isostructural. The $c\beta$ phase of the other lanthanide fluoride system studied, M = Tm, was indexed on rhombohedral rather than cubic symmetry (18). Greis suggested that these cubic $c\beta$ phases should be considered an intergrowth of the corresponding $M_{14}F_{33}$ and $M_{13}F_{31}$ phases, both of which were observed as polycrystals in the binary systems. The lattice parameters for these fluoride phases are much smaller than that for $Ba_{17}Sm_{10}Cl_{64}$ phase: for M = Sm, a = 17.423 Å; M = Eu, a = 17.342 Å; M = Sr/Eu, a = 17.296 Å; and M = Yb, a = 16.712 Å.

In addition to a table of the fluorite-related reflections and their intensities, Greis included a line diagram of the

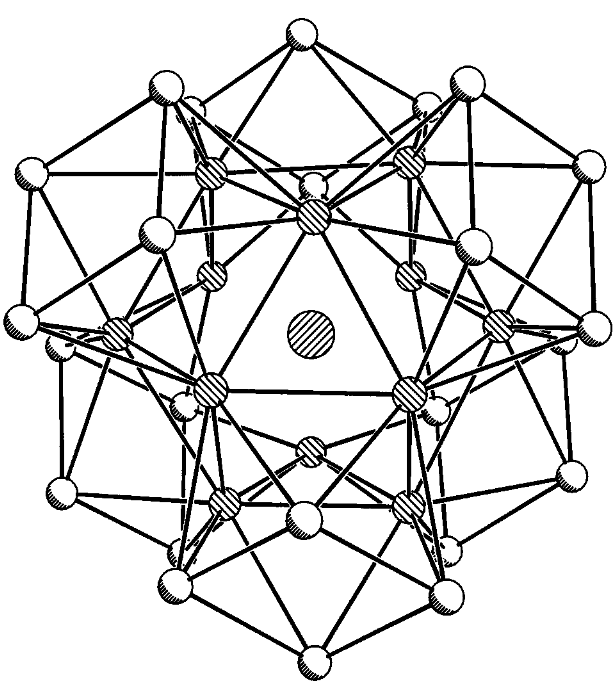

FIG. 4. A projection of the $BaSm_5Cl_{37}$ cluster down the 3-fold axis. Only Cl atom positions are shown.

$YbF_{2.37}$ powder pattern from which we could determine approximate *d* values, but not intensities, of nonfluorite reflections (17). We calculated the X-ray powder diffraction pattern for $YbF_{2.37}$ (19) using the atomic coordinates reported for $Ba_{17}Sm_{10}Cl_{64}$, temperature factors of 0.5 for the Yb atoms and 1.0 for the fluorine atoms, a lattice parameter of 16.712 Å (17), and scattering factors for Yb^{2+} replacing Ba^{2+}, Yb^{3+} replacing Sm^{3+}, and F^{1-} replacing Cl^{1-}. The simulated pattern reproduces all 14 observed reflections and includes only 3 unobserved reflections with calculated intensities of 2, 3, and 1. Although the Ba^{2+} ion (1.42 Å) is significantly larger than the Yb^{2+} ion (1.19 Å) (20), the simulated powder pattern agrees surprisingly well with that reported and suggests strongly that the $c\beta$ phase is isostructural with $Ba_{17}Sm_{10}Cl_{64}$.

In addition, Wang and Grey (21) studied the $Ca_{1-x}Y_xF_{2+x}$ ($x = 0.03$–0.32) system by solid state ^{19}F magic-angle spinning NMR and concluded that the cubic fluorite structure accommodates the increasing concentration of the F^{1-} ions by increasing the concentration of cuboctahedrons in the structure. The structure we propose for the $c\beta$ ($YbF_{2.37}$) phase is consistent with their conclusions.

ACKNOWLEDGMENT

Help provided by Dr. Donald Ward in collecting the data is acknowledged gratefully.

REFERENCES

1. R. Blachnik, G. Alberts, and E. Enninga, *Z. Anorg. Allg. Chem.* **522,** 207–216 (1985).
2. U. Löchner and R. Blachnik, *Z. Kristallogr.* **183,** 207–212 (1988).
3. D. J. M. Bevan, O. Greis, and J. Strähle, *Acta Crystallogr. A* **36,** 889–890 (1980).
4. H. Bärnighausen, J. M. Friedt, and J. P. Sanchez, Poster DP39 (Abstracts p. 31), Rare Earth Res. Conf., Zürich, 1985.
5. G. Meyer and S. Masselmann, *Chem. Mater.* **10,** 2994–3004 (1998).
6. See, for example, G. Liu and H. A. Eick, *J. Less-Common Met.* **149,** 47–53 (1989).
7. G. Liu and H. A. Eick, *Inorg. Chem.* **27,** 2161–2163 (1988).
8. G. M. Sheldrick, "SHELX-92, Program for the Refinement of Crystal Structures." University of Göttingen, Germany, 1993. [Structural solution effected with Siemens SHELXTL PC software package (release 4.2, 1991).]
9. D. J. M. Bevan, M. J. McCall, S. E. Ness, and M. R. Taylor, *Eur. J. Solid State Inorg. Chem.* **25,** 517–526 (1988).
10. D. J. M. Bevan, J. Strähle, and O. Greis, *J. Solid State Chem.* **44,** 75–81 (1982).
11. D. J. M. Bevan, S. E. Ness, and M. R. Taylor, *Eur. J. Solid State Inorg. Chem.* **25,** 527–534 (1988).
12. M. Eitel, Ph.D. dissertation, Universität Karlsruhe, Germany, 1985.
13. S. Masselmann and G. Meyer, *Z. Anorg. Allg. Chem.* **625,** 1–2 (1999).
14. M. S. Wickleder, P. Egger, T. Riedener, N. Furer, H. U. Güdel, and J. Hulliger, *Chem. Mater.* **8,** 2828–2831 (1996).
15. O. Greis, *J. Solid State Chem.* **24,** 227-232 (1978).
16. O. Greis, *Z. Anorg. Allg. Chem.* **441,** 39–46 (1978).
17. O. Greis, *Z. Anorg. Allg. Chem.* **430,** 175–198 (1977).
18. O. Greis and T. Petzel, *Z. Anorg. Allg. Chem.* **434,** 89–94 (1977).
19. W. Lasocha and K. Lewinski, Program LAZY PULVERIX, *in* "Program PROSZKI—A System of Programs for Powder Diffraction Data Processing," Jagiellonian University, 30–060 Krakow, Poland, private communication.
20. R. D. Shannon, *Acta Crystallogr. A* **32,** 751–67 (1976).
21. F. Wang and C. P. Grey, *Chem. Mater.* **10,** 3081–3091 (1998).